

# Image Analysis for Obturator Foramen Based on Marker-Controlled Watershed Segmentation and Zernike Moments

Seda Sahin, Emin Akata

**Abstract**—Obturator Foramen is a specific structure in Pelvic bone images and recognition of it is a new concept in medical image processing. Moreover, segmentation of bone structures such as Obturator Foramen plays an essential role for clinical research in orthopedics. In this paper, we present a novel method to analyze the similarity between the substructures of the imaged region and a hand drawn template as a preprocessing step for computation of Pelvic bone rotation on hip radiographs. This method consists of integrated usage of Marker-controlled Watershed segmentation and Zernike moment feature descriptor and it is used to detect Obturator Foramen accurately. Marker-controlled Watershed segmentation is applied to separate Obturator Foramen from the background effectively. Then, Zernike moment feature descriptor is used to provide matching between binary template image and the segmented binary image for final extraction of Obturator Foramen. Finally, Pelvic bone rotation rate calculation for each hip radiograph is performed automatically to select and eliminate hip radiographs for further studies which depend on Pelvic bone angle measurements. The proposed method is tested on randomly selected 100 hip radiographs. The experimental results demonstrated that the proposed method is able to segment Obturator Foramen with 96% accuracy.

**Keywords**—Medical image analysis, marker-controlled watershed segmentation, segmentation of bone structures on hip radiographs, pelvic bone rotation rate, zernike moment feature descriptor.

## I. INTRODUCTION

IMAGE processing techniques has been extensively used in medical image analysis with an increasing success. Anatomical bone structure segmentation and feature extraction from different bone structures are fundamental concepts for this study. Geometric measurements which are based on Pelvic bone structures and especially shape features for Obturator Foramen play important roles in clinical research in orthopedics. The position of Pelvic bone structure at hip radiograph is measured by Pelvic bone rotation rate. It is defined with the ratio of diameter of Obturator Foramen of right side and diameter of Obturator Foramen of left side of Pelvic bone structure [1], [2]. Accurate measurement for Pelvic bone rotation has a significant role in the acetabular angle measurements in treatment of Pelvic bone diseases. It is used as a preprocessing step to select and eliminate images which can be used for measurements on Pelvic bone structure

later. Moreover, automatic measurement of this rate gains speed and time to clinician.

Generally, medical image segmentation is the determination of region of interest for anatomical structures with respect to some anatomical features and additionally is a distinguishing process for these regions from the background. There are several types of segmentation techniques which can be defined as region-based segmentation techniques (Thresholding, Region growing, Watershed segmentation, Clustering algorithms) and edge-based segmentation techniques (Gradient operators, Graph searching, Contour following). They can also be classified as manual/semiautomatic/ full automatic segmentation [3], [4]. The chosen segmentation technique proved to fit best to the aim of the study and relevant images of it. Pelvic bone structure detection from hip radiographs has been studied frequently on femoral head and acetabulum. However, Obturator Foramen segmentation and feature extraction for this structure on hip radiographs are new concepts for medical image analysis.

In medical imaging, Watershed segmentation method is preferred frequently to segment different types of anatomical structures and tissues due to its advantages such as simplicity, high speed. Its main disadvantage is oversegmentation problem which is solved with Marker-based Watershed segmentation [5]-[8]. There are several shape and feature descriptors in the literature. Zernike moment feature descriptor is required for general shape applications due to robust and accurate shape description, fast computation, image noise sensitivity and rotation invariance properties [9]-[13].

In this paper, we proposed a new segmentation method for the extraction of Obturator Foramen with integrated usage of Marker-based Watershed segmentation method and Zernike moment feature descriptor. The Marker-based Watershed segmentation is applied to region of interest image (ROI) which is pointed out manually by clinician as a first step. Then, Zernike moment feature descriptor is applied to these segmented images and binary template image separately to extract amplitude and phase features of them. Additionally, the diameters of Obturator Foramen of the segmented binary images are compared with the diameter of Obturator Foramen of the binary template image which is "neutral Pelvic rotation image" and then the incompatible images are eliminated. Thus, the similarity between template image and segmented images can be detected to select the usable images which satisfy normal limits for Pelvic bone rotation rate. Then, Pelvic bone rotation rate (Pbrr) measurement is performed

Seda Sahin and Emin Akata are with the Department of Electrical and Electronics Engineering, Baskent University, Ankara, Turkey (e-mail: SedaSahinmail@gmail.com, akata@baskent.edu.tr).

automatically. This automatic Pelvic bone rotation measurement system contributes clinician workload considerably and prevents time-consuming process for large datasets. On the other hand, it constitutes a preprocessing step for determination of images which can be used for acetabular angle measurements on Pelvic bone structure on hip radiographs.

## II. PROPOSED SYSTEM

The proposed system is an automated Pelvic bone rotation rate measurement system and it consists of basically three stages. The proposed system is described in Fig. 1.

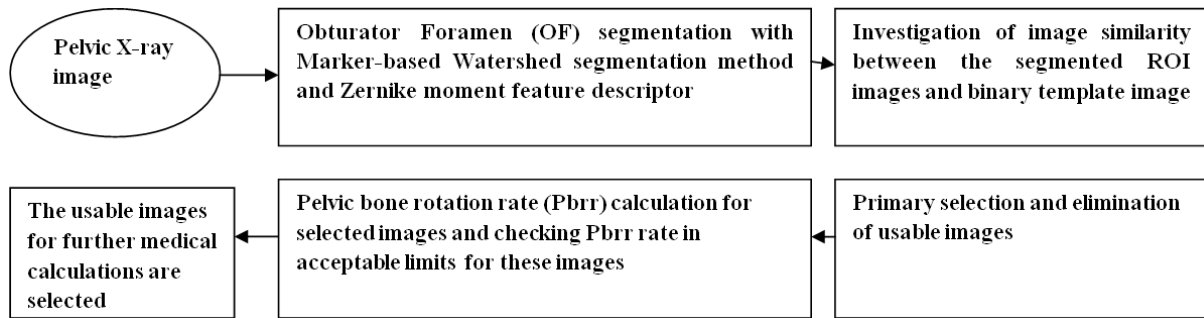


Fig. 1 Automated Pelvic bone rotation rate (Pbrr) measurement system

### A. STEP 1: Segmentation of Obturator Foramen

The first step of the proposed system consists of the application of the new segmentation method for Obturator Foramen and extraction of segmented ROI images. These segmented ROI images are obtained by separation of region of Obturator Foramen from the other parts of the Pelvic bone image. The segmentation method for region of left and right Obturator Foramen consists of basically 2 steps that are described in Fig. 2.

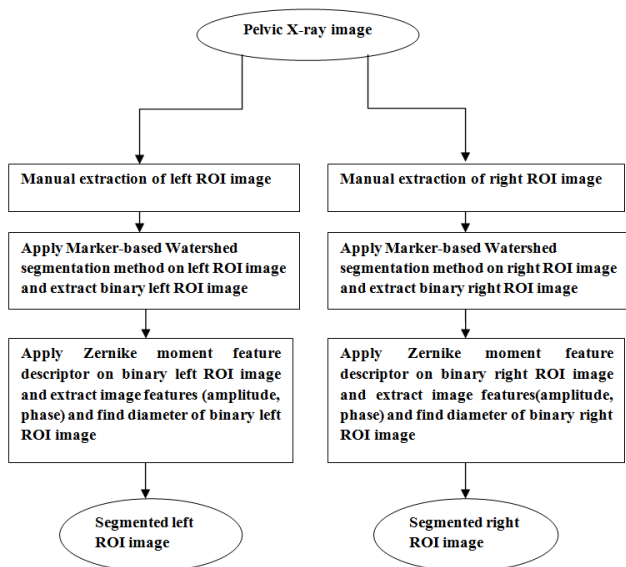


Fig. 2 The proposed segmentation method chart

Initially, the ROI images to be processed are determined with manual extraction of clinician for both left and right part of hip radiograph, as shown in Figs. 3 and 4.



Fig. 3 Pelvic X-ray image

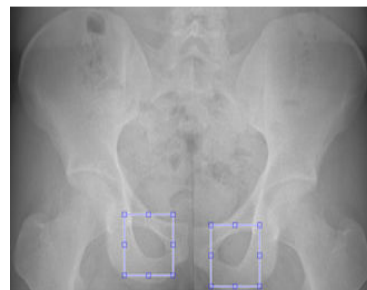


Fig. 4 The left/right ROI image

The first step of the proposed segmentation method is the application of Marker-based Watershed segmentation (MbWs) method on ROI images. Generally, Watershed segmentation method is based on the idea of application of some morphological operations with region growing method. The image is considered as a topographic structure and height of each point is defined as its gray level, then this structure is fallen on by rain and the lakes are defined as “catchment basins” and the lines that separate these lakes are defined as “watershed lines”. This method is used on the gradient of the image and the gradient boundaries are considered as region separation boundaries which distinguish foreground parts of the image from background parts of the image. On the other hand, oversegmentation problem is the main disadvantage of

the Watershed segmentation method and MbWs is used to overcome this oversegmentation problem with addition of foreground and background markers onto the image. The markers are used automatically on ROI images and binary template image in this study. The center of shape of Obturator Foramen is defined as foreground marker and the markers which are placed on the four corners of ROI image are defined as background markers. The Watershed segmentation method is applied on gradient of ROI image by region growing from the markers. The foreground region of binary ROI image is defined as binary 1 (white) as shape of Obturator Foramen and the background region of binary ROI image is represented as binary 0 (black) after application of the Watershed segmentation. Sample representation of automatic marker selection for ROI image and application of MbWs over these markers are shown in Fig. 5.

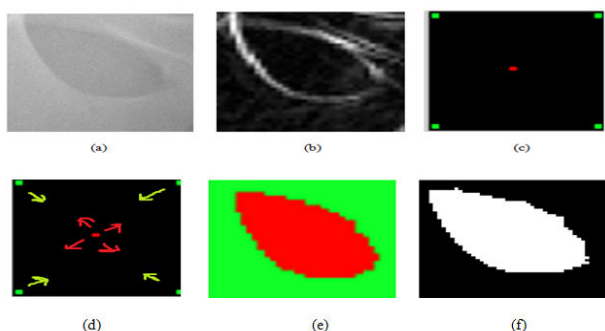


Fig. 5 (a) The left ROI image (b) Gradient image (c) representation of foreground and background markers for ROI image (d) application of region growing from markers (e) result of MbWs (f) binary image representation of (e)

Sample representation of application of MbWs on the left ROI image and the right ROI image are shown in Figs. 6 (b) and (c), in Figs. 7 (b) and (c) respectively.

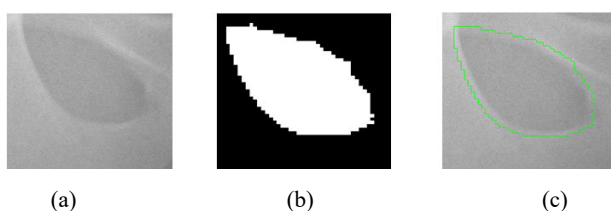


Fig. 6 Samples of MbWs results for the left ROI image (a) The left ROI image (b) MbWs result of the left ROI image (c) grey level representation of MbWs result of the left ROI image

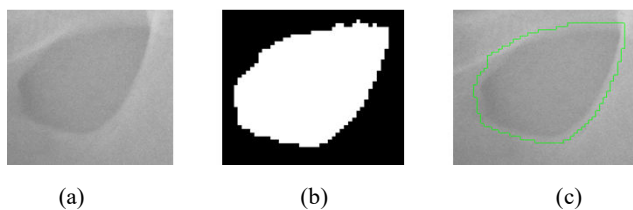


Fig. 7 Samples of MbWs results for the right ROI image (a) The right ROI image (b) MbWs result of the right ROI image (c) grey level representation of MbWs result of the right ROI image

The second step of the proposed segmentation method is the application of Zernike moment feature descriptor (Zmfd) on ROI images. Zernike moment feature descriptor is applied to these segmented images and binary template image separately to extract features (amplitude (A), phase ( $\phi$ )) of them. These features are used to determine similarity between binary template image and candidate segmented ROI images. Since Zernike moments are invariant to rotation and possess various orthogonality properties, they are used frequently in various image analysis applications. Zernike moments are defined as mapping of an image onto a set of complex Zernike polynomials which form a orthogonal set over the interior of the unit circle and these polynomials are orthogonal [9]-[13]. Radial polynomials ( $Rn,m$ ) are defined in (1).

$$Rn,m = \sum_{s=0}^{(n-|m|)/2} (-1)^s \frac{(n-s)!}{s!((n+|m|)/2-s)!((n-|m|)/2-s)!} \rho^{n-2s} \quad (1)$$

where n represents the order of the radial polynomial and it is a nonnegative integer, m is a positive or negative integer which is related with the representation of the repetition of the azimuthal angle and it must satisfy  $n - |m| = \text{even}$  and  $|m| \leq n$  conditions. The length of the vector from the origin to (x,y) is defined as  $\rho$ .

Zernike basis functions ( $Vn,m$ ) are defined in (2).

$$Vn,m(\rho, \theta) = Rn,m(\rho)e^{jm\theta}, |\rho| \leq 1 \quad (2)$$

Zernike polynomials ( $Zn,m$ ) have orthogonality property and they are represented in (3).

$$\int_0^{2\pi} \int_0^1 V^*_{n,m}(\rho, \theta) V_{p,q}(\rho, \theta) \rho d\rho d\theta = \begin{cases} \frac{\pi}{n+1} & n=p, m=q \\ 0 & \text{otherwise} \end{cases} \quad (3)$$

Finally, Complex Zernike moments are defined in (4).

$$Zn,m = \frac{n+1}{\pi} \int_0^{2\pi} \int_0^1 f(\rho, \theta) V^*_{n,m}(\rho, \theta) \rho d\rho d\theta \quad (4)$$

where  $f(c,r)$  image function has  $f(\rho, \theta)$  polar form and \* represents the complex conjugate. In (4), the integrals are replaced with summations for computation of Zernike moments of NxN digital image and a mapping transform is used to normalize the coordinates of this image. This process is defined in (5).

$$Zn,m = \frac{n+1}{\lambda_N} \sum_{c=0}^{N-1} \sum_{r=0}^{N-1} f(c,r) V^*_{n,m}(c,r) = \frac{n+1}{\lambda_N} \sum_{c=0}^{N-1} \sum_{r=0}^{N-1} f(c,r) Rn,m(\rho_{cr}) e^{-jm\theta_{cr}} \quad (5)$$

where the normalization factor  $\lambda_N$  which are the number of pixels in the unit circle  $\pi$  and  $0 \leq \rho \leq 1$  then  $\rho_{cr}$  (transform distance) and  $\theta_{cr}$  (phase) are defined in (6).

$$\rho_{cr} = \frac{\sqrt{(2c-N+1)^2 + (2r-N+1)^2}}{N} \quad \phi = \theta_{cr} = \tan^{-1} \frac{(N-1-2r)}{(2c-N+1)} \quad (6)$$

$|Zn,m|$  = amplitude (A) = magnitude of Zernike moments

The mapping process which is used to normalize the coordinates of  $N \times N$  digital image is shown in Fig. 8.

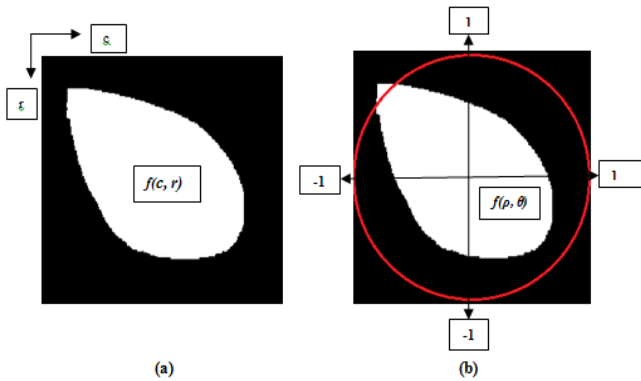


Fig. 8 (a)  $N \times N$  (260 pixel x 260 pixel) The left binary template image with function  $f(c, r)$  (b) The left binary template image is mapped onto the unit circle with function  $f(\rho, \theta)$

In this study, the magnitudes of Zernike moments are used as fundamental features which determine the Obturator Foramen. Also, the phase and diameter information are used as other features to detect similarity between template image and segmented ROI images. Sample representation of application of Zernike moment feature descriptor on the left ROI image and the right ROI image are shown in Figs. 9 (c) and 10 (c) respectively. Application of Zernike moment feature descriptor on the left binary template image and the right binary template image are shown in Figs. 11 (b) and 12 (b) respectively.

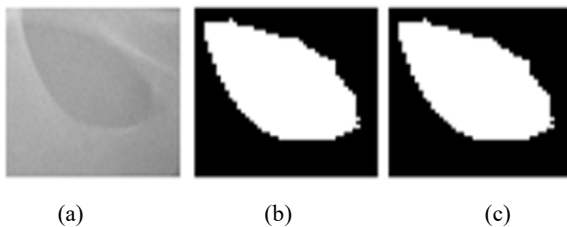


Fig. 9 Zmfd result for the left ROI image (a) The left ROI image (b) MbW's segmentation result for (a) (c) Zmfd result for (b) ( $A=0.17$ ,  $\phi=110.95$  degree)

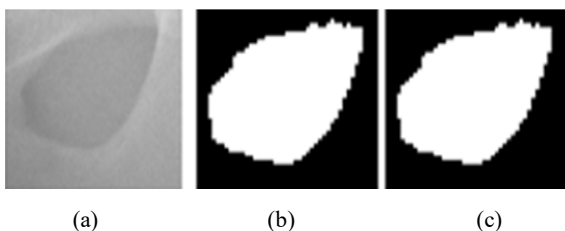


Fig. 10 Zmfd result for the right ROI image (a) The right ROI image (b) MbW's segmentation result for (a) (c) Zmfd result for (b) ( $A=0.10$ ,  $\phi=79.26$  degree)



Fig. 11 Zmfd result for the left binary template image (a) The left binary template image (b) Zmfd result for (a) ( $A=0.18$ ,  $\phi=100.35$  degree)



Fig. 12 Zmfd result for the right binary template image (a) The right binary template image (b) Zmfd result for (a) ( $A=0.18$ ,  $\phi=80.65$  degree)

### B. STEP 2: Segmented ROI Image Feature Analysis and Evaluation

The second step is to search image similarity between the segmented ROI images and binary template image with respect to image features (amplitude, phase, and diameter). The amplitude and phase features of segmented images and binary template images are obtained with application of Zernike moment feature descriptor. On the other hand, the diameter of Obturator Foramen is defined as FL (Obturator Foramen Length) which is represented in Fig. 13.

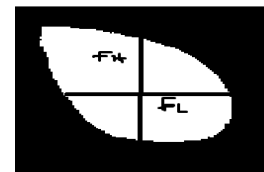


Fig. 13 Obturator Foramen length (FL) and Obturator Foramen height (FH) representation

Primary elimination and selection of usable images are performed with respect to the similarities between amplitude, phase, and diameter features of left/right ROI images and left/right binary template images. The diameter features for segmented ROI images are extracted with MATLAB *minor axis length function*. This function gives results in terms of pixel. The conversion between pixel to centimeter is achieved by approach of the width for 260 x 260 pixels image is 6,5 cm and 1 pixel is 0,02cm (6,5 cm/260 pixels) [14]. Sample representation of application of Zernike moment feature descriptor on the left binary template image and the right binary template image with diameter features are shown in Figs. 14 (a) and (b). Additionally, application of Zernike moment feature descriptor on the left ROI image and the right ROI image are shown with diameter features in Figs. 15 (a) and (b).



Fig. 14 (a) Zmfd result ( $A=0.18$ ,  $\phi=100.35$  degree) and diameter of the left binary template image: 2.76 cm (b) Zmfd result ( $A=0.18$ ,  $\phi=80.65$  degree) and diameter of the right binary template image: 2.76 cm



Fig. 15 (a) Zmfd result ( $A=0.17$ ,  $\phi=110.95$  degree) and diameter of the left ROI: 2.72 cm (b) Zmfd result ( $A=0.10$ ,  $\phi=79.26$  degree) and diameter of the right ROI: 3.2 cm

**C. STEP 3: Pelvic Bone Rotation Rate Calculation (Pbrr)**

The last step is the calculation of Pelvic bone rotation rate (Pbrr) automatically. This rate is checked for the acceptable medical limits which are between 0.56 and 1.8. Thus, usable images which can be used for acetabular angle measurements on Pelvic bone structure on hip radiographs are selected. In Figs.16 and 17, the diameter of the left binary template image (LD) and the diameter of the right binary template image (RD) are shown. These hand drawn templates are used as golden standard images to provide "neutral Pelvic rotation image" condition ( $Pbrr=1$ ) and searching similarity between images.

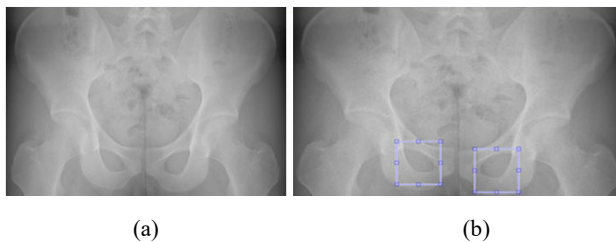


Fig. 16 (a) Pelvic X-ray image, (b) The left/right ROI image

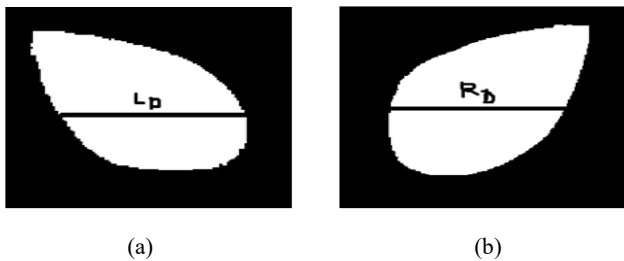


Fig. 17 (a) Diameter of the left binary template image: 2.76 cm, (b) Diameter of the right binary template image: 2.76 cm

Automatic Pelvic bone rotation rate is defined as follows:

$$Pbrr = RD / LD$$

Pbrr rate must be in acceptable limits (0.56-1.8) and the calculation for this rate is based on similarity of diameter feature between template images and segmented ROI images. Then, the last selection of usable images for further medical calculations is performed after checking Pbrr rate which is in acceptable limits.

**III. EXPERIMENTAL RESULTS**

In this study, the segmentation performance of the proposed method is evaluated by objective evaluation in terms of accuracy [15], [16].

$$Accuracy = TP + TN / TP + TN + FP + FN$$

where **TP**: True Positive, **TN**: True Negative, **FP**: False Positive, **FN**: False Negative. In Figs. 18 and 19, FP, TP, FN representation which is used to compare the proposed method and manual method is shown. The intersection of the proposed method (green line) and manual segmentation by clinician (black line) is demonstrated as TP, the segmentation results which are produced only by the clinician is demonstrated as FN and the segmentation results which are produced only by the proposed method is demonstrated as FP in Fig. 19 (c).

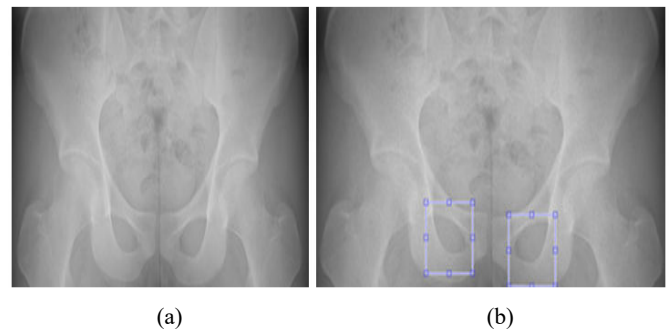


Fig. 18 (a) Pelvic X-ray image (b) The left/right ROI image

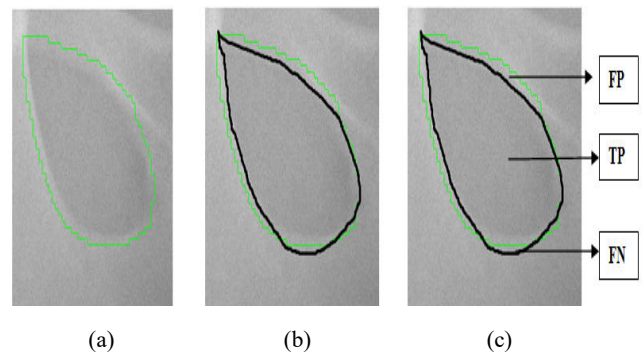


Fig. 19 Segmentation performance evaluation (a) Final segmentation result (b) The ROI image which is marked by clinician (c) FP, TP, FN representation to compare (a) and (b)

The proposed segmentation method is tested on randomly selected 100 hip radiographs (Pelvic X-ray images) and is implemented in MATLAB. Segmentation performance of this

method is based on comparison between the manual segmentation results of ROI images and segmentation results for the proposed method. The results of proposed method are shown as green lines and manual segmentation results are demonstrated as black lines on sample ROI images in Fig. 20. It can be seen that the contours for the proposed method and manual method are closed to each other and so the effectiveness of the proposed method is confirmed. Additionally, segmentation performance of the proposed segmentation method in terms of accuracy for sample Pelvic X-ray images are shown in Table I. The experimental results which are obtained from 100 hip radiographs represent that our method is able to segment Obturator Foramens with % 96 accuracy. Although, the execution time for the manual segmentation is approximately 20 seconds for each ROI image, the execution time for the proposed method is approximately 0,2 seconds for each ROI image. These results demonstrate effectiveness of the proposed method, too.

TABLE I  
SEGMENTATION PERFORMANCE OF THE PROPOSED METHOD IN TERMS OF ACCURACY FOR SAMPLE PELVIC X-RAY IMAGES

Pelvic X-ray image	Accuracy for left ROI image	Accuracy for right ROI image
Img1	0.93	0.98
Img2	0.95	0.93
Img3	0.97	0.92
Img4	0.98	0.99
Img5	0.96	0.97
Img6	0.97	0.95
Img7	0.96	0.97
Img8	0.97	0.96
Img9	0.95	0.96
Img10	0.96	0.98

#### IV. CONCLUSION

In this study, we have proposed a new segmentation method to determine boundary of Obturator Foramen which is based on integrated usage of Marker-Based Watershed segmentation method and Zernike moment feature descriptor. In addition, an automatic Pelvic Bone rotation measurement system is developed by using feature of diameter of Obturator Foramen. The segmentation method is tested on randomly selected 100 hip radiographs. We have demonstrated that all tested Obturator Foramens are detected with %96 accuracy. Moreover, this study is focused on the similarity between the segmented binary ROI images and binary template image to perform reliable Pelvic bone rotation measurements and to select images which have "acceptable rotational rate" for further studies on Pelvic bone structure angle measurements. In conclusion, this automated Pelvic bone rotation measurement system prevents time consuming to choose processing images for further angle measurements which are based on Pelvic bone structure.

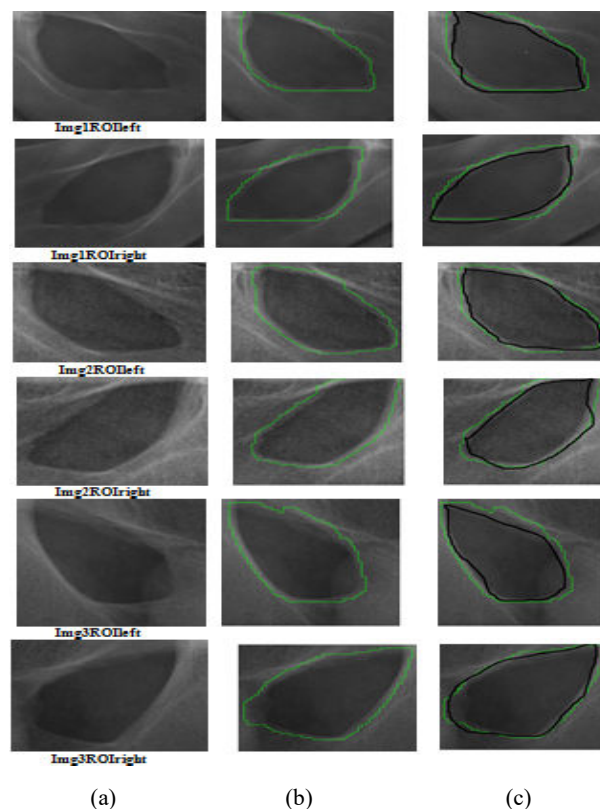


Fig. 20 (a) Sample ROI images (b) Proposed segmentation method results of ROI images (green lines) (c) The ROI images which are segmented by clinician (black lines)

#### REFERENCES

- [1] F. G. Boniforti, G. Fujii, R. D. Angliss, M. K. D. Benson, "The reliability of measurements of Pelvic Radiographs in infants", *J Bone Joint Surg (Br)*, vol. 79-B, no. 4, pp. 570-575, 1997.
- [2] D. Tönnis, "Normal values of the hip joint for the evaluation of X-rays in children and adults", *Clinical Orthopaedics*, vol. 119, pp. 39-47, 1976.
- [3] I. N. Bankman, *Handbook of Medical Imaging*, Academic Press, 2000.
- [4] R. C. Gonzalez, R. E. Woods, *Digital Image Processing*, Second Edition, Prentice Hall, 2002.
- [5] X. Zhang, F. Jia, S. Luo, G. Liu, Q. Hu, "A marker-based watershed method for X-ray image segmentation", *Computer Methods And Programs in Biomedicine*, vol. 113, pp. 894-903, 2014.
- [6] S.S. Kumar, R.S. Moni, J. Rajeeesh, "Automatic Segmentation of Liver and Tumor for CAD of Liver", *Journal of Advances in Information Technology*, vol. 2, issue1, 2011.
- [7] J. Mehena, M. C. Adhikary, "Brain Tumor Segmentation and Extraction of MR Images Based on Improved Watershed Transform", *IOSR Journal of Computer Engineering*, vol. 17, issue 1, pp. 1-5, 2015.
- [8] A. W. Reza, C. Eswaran, K. Dimiyati, "Diagnosis of Diabetic Retinopathy: Automatic Extraction of Optic Disc and Exudates from Retinal Images using Marker-controlled Watershed Transformation", *J Med Syst*, vol. 35, pp. 1491-1501, 2011.
- [9] S. W. Foo, Q. Dong, "A Feature-based Invariant Watermarking Scheme Using Zernike Moments", *World Academy of Science, Engineering and Technology*, vol. 4, 2010.
- [10] A. Tahmasbi, F. Saki, S. B. Shokouhi, "Classification of benign and malignant masses based on Zernike moments", *Computers in Biology and Medicine*, vol. 41, pp. 726-735, 2011.
- [11] F. Saki, A. Tahmasbi, H. Soltanian-Zadeh, S. B. Shokouhi, "Fast opposite weight learning rules with application in breast cancer diagnosis", *Computers in Biology and Medicine*, vol. xx, pp., 2012.
- [12] M. Zhenjiang, "Zernike moment-based image shape analysis and its application", *Pattern Recognition Letters*, vol. 21, pp. 169-177, 2000.

- [13] S. Sharma, P. Khanna, "Computer-Aided Diagnosis of Malignant Mammograms using Zernike Moments and SVM", *J Digit Imaging*, vol.28, pp. 77-90, 2015.
- [14] A. E. Villafuerte-Nuñez, A. C. Téllez-Anguiano, O. Hernández-Díaz, R. Rodríguez-Vera, J. A. Gutiérrez-Gnecchi, J. L. Salazar-Martínez, "Facial Edema Evaluation Using Digital Image Processing", *Hindawi Publishing Corporation, Discrete Dynamics in Nature and Society*, Volume 2013, Article ID 927843, 2013.
- [15] T. Fawcett, "An introduction to ROC Analysis", *Pattern Recognition Letters*, vol. 27, pp. 861-874, 2006.
- [16] J. Bozek, M. Mustra, K. Delac, M. Grgic, "A Survey of Image Processing Algorithms in Digital Mammography", *Rec.Advan. in Mult. Sig. Process. and Commun.*, SCI 231, pp. 631-657, 2009.

**Seda Sahin** received her B.S degree in Computer Engineering from Eastern Mediterranean University, Famagusta, North Cyprus in 2003 and received her M.S degree in Computer Engineering from Çankaya University, Ankara, Turkey in 2006. Currently, she is a PhD student with the Department of Electrical and Electronics Engineering, Baskent University, Ankara, Turkey. Her research interests include image processing, telecommunication systems, expert systems.

**Emin Akata** received his B.S degree in Electrical Engineering from METU, Ankara, Turkey in 1968, M.S. degree in Electrical Engineering from METU in 1970 and Ph.D. degree in Computer Engineering from Hacettepe University, Ankara, Turkey in 1982 respectively. He is a Professor with the Department of Electrical and Electronics Engineering, Baskent University, Ankara, Turkey and he is chairman of the Department of Electrical and Electronics Engineering and director of Institute of Science and Engineering. His research interests include image processing, digital electronics and computer architecture.